Latin American Journal of Solids and Structures
www.lajss.org

Quasi-static numerical study of the breathing mechanism of an elliptical crack in an unbalanced rotating shaft

Abstract

In this paper we present the numerical analysis of the quasi-static behavior of an unbalance cracked shaft with straight and elliptical cracks considering an eccentric mass. The rotation of the shaft has been simulated by considering different angular positions to complete one rotation. The influence of the mass eccentricity in the opening of the crack has been studied considering different angles of eccentricity. The study of the partially opening/closing of the crack in the rotation of the shaft under the influence of the eccentric mass is analyzed. The work allows us to know the influence of the unbalance in the crack breathing mechanism and will help to predict the influence of this behavior on the values of the Stress Intensity Factor and on the propagation of cracks.

Keywords

Breathing mechanism, Rotating Shaft, Elliptical crack, Eccentricity, Rotating machinery.

Lourdes Rubio [a]
Belén Muñoz-Abella [b]
Patricia Rubio [c]
Laura Montero [d]

Department of Mechanical Engineering
University Carlos III of Madrid
[a] lrubio@ing.uc3m.es
[b] mmunoz@ing.uc3m.es
[c] prubio@ing.uc3m.es
[d] lamonter@ing.uc3m.es

Received 03.09.2013
In revised form 20.05.2014
Accepted 20.06.2014
Available online 16.08.2014

1 INTRODUCTION

The failures of machines are produced quite often by the presence and propagation of fatigue cracks due to the loads and solicitations they carry. Those failures sometimes are catastrophic and produce personal injuries or economic problems. The increasing importance of safety and costs derived from failure in machinery has pushed the researchers in the field of damage detection to analyze the behavior of mechanical components with defects.

Shafts, that are one of the main components of machines, perform in rotation and, due to the applied loads, bending and torsion efforts appear during the work. This behavior together with the

mass unbalances, very much frequent and the most common source of vibrations in shafts, can produce the shaft failure by generation and propagation of fatigue cracks.

In the presence of a crack, when a shaft rotates, the crack opens and closes once per revolution. The opening and closing of the crack has been modeled in different ways. The simplest one is to consider that the crack is always open (Papadopoulos and Dimarogonas (1987), Zhou et al. (2005) and Papadopoulos (2008), among others), or that the crack is open or closed, so that the crack is half the rotation in the open state and the other half in the closed one. This model, commonly called "switching" model has been used quite often i.e by Gasch (1976), Muller et al. (1994), Pu et al. (2002), Qin et al. (2003), Qin et al. (2004), Gasch (2008) due to its simplicity. However the most feasible behavior of the crack is that called the "breathing" behavior. In this case, the crack passes from the closed state to the open state gradually in a rotation. The crack is closed when it is situated in the compression zone of the shaft and it is open when situated in the tensile zone. The transition between both situations produces partial opening or closing of the crack when the static deflection dominates the performance of the rotating shaft. The partial opening/closing of the crack has been studied, numerically or analytically, by different authors: Jun et al. (1992), Dimarogonas and Papadopoulos (1983), Darpe et al. (2004), Papadopoulos (2004), Patel and Darpe (2008), Bachschmid et al. (2008), Al-Shudeifat and Butcher (2011) or more recently by Morais et al. (2012), always considering an aligned and balanced shaft, although recent works pointed out in the direction of considering the breathing of crack in unbalanced shafts, see for example the works of Patel et al. (2011), Kulesza and Sawicki (2012), Rubio et al. (2012) and Munoz et al. (2012). The opening and closing of the crack is very much influenced by the values taken by the Stress Intensity Factor (SIF) at the crack front as the shaft rotates. The crack is open while the SIF at the front remains positive, otherwise the crack will be closed.

In the real performance of shafts it is very usual that the shafts present unbalances or misaligments that modify the normal behavior of the component. A very common unbalance of shafts is due to the presence of eccentric masses: Sekhar and Prabhu (1998), Darpe et al. (2004), Patel and Darpe (2008), Qingkai et al. (2010), Gyekenyesi et al. (2010), Cheng et al (2011) and Kulesza and Sawicki (2012). The unbalance, as mentioned before, modifies the dynamic behavior of the rotating shafts and may hide the presence of the cracks or, on the other hand, can increase their effects.

Most of the aforementioned studies consider straight front cracks, and are less frequent those analyzing elliptical front shapes (Couroneau and Royer (1998), Carpinteri et al. (1998), Shin and Cai (2004), Rubio et al. (2011)), although this is the type of cracks in real cracked shafts.

The study of the dynamic behavior of cracked shafts has been carried out in the last few decades using different models. The most popular and widely used is the Jeffcott rotor model used by Jun et al. (1992), Penny and Friswell (2002), Gómez-Mancilla et al. (2004), Darpe et al. (2006), Darpe (2007), Patel and Darpe (2008), Gyekenyesi et al. (2010), Cheng et al. (2011) among others. It consists of a simply supported shaft with a disc at the midspan. Despite its simplicity, this model allows us to analyze the effects of cracks and other defects such as misalignment or unbalances and, as Ishida (2008) pointed out, it permits to explain the behavior of industrial cracked rotors.

In this paper we present the quasi-static numerical study of the influence of the eccentricity in a rotating cracked shaft using a finite element model of the cracked Jeffcott rotor. No results of this kind have been found in the literature, in the knowledge of the authors. The model includes the

presence of an elliptical crack. The analysis has been made using the commercial finite element code ABAQUS/Standard (2007). We present the comparison, for each angle of rotation, of the partially opening/closing of the crack for different positions of the eccentricity. The work allows us to know the influence of the unbalance of rotating shafts in the crack breathing mechanism and allows us to predict the influence of this behavior on the values of the Stress Intensity Factor and in the propagation of elliptical cracks.

2 FINITE ELEMENT MODEL OF A CRACKED SHAFT

The numerical simulation of the problem has been carried out using a commercial code of the Finite Element Method (ABAQUS©/Standard) (2007). For this analysis, the complete 3D model of the shaft has been considered due to there is no symmetry in the evaluated problem. The structured mesh of the three dimensional model is made employing a type of elements called C3D8R (8-node linear brick, reduced integration) in ABAQUS nomenclature. The mesh has been refined up to a size of elements for which the convergence of results was achieved by means of a mesh sensitivity analysis. In order to get more accurate results, the mesh presents more density near the crack in the length direction and around the crack front as can be seen in Figure 1. The final number of elements is close to 200.000 elements.

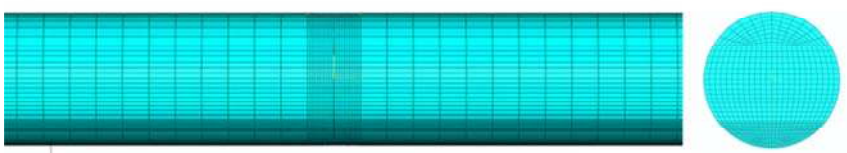


Figure 1: Example of mesh of the model in longitudinal and transversal direction.

The numerical model has been made in such a way that a surface-to-surface contact interaction has been defined between the crack faces in order to avoid the interpenetration between them, during the closing. To complete the definition of the contact model it is necessary to establish both normal and tangential properties between the crack faces. Regarding to the normal properties, "hard" contact is used. This relationship does not allow the penetration of the surfaces in contact at the constraint locations and prevents the transfer of tensile stress across the interface. The chosen tangential property, "rough" friction, introduces an infinite coefficient of friction that avoids all relative sliding motion between the two contacting surfaces.

As for many other studies on rotordynamics like Penny and Friswell (2002), Darpe et al. (2006), Darpe (2007), Jun and Gadala (2008), Patel and Darpe (2008) and Cheng et al. (2011), the classical Jeffcott rotor model has been chosen for this analysis. This simple but useful model consists in a massless shaft simply supported at the ends, with a disc at the midspan to simulate a concentrated mass. The crack, of length a is situated also at the midspan of the shaft having a straight or elliptical front oriented on a plane normal to the axis of the shaft (Figure 2a)). The round bar total length is equal to 900mm, whereas the diameter is D=20 mm. The material of the shaft is aluminum with the following mechanical properties: Young's Modulus E=72GPa, Poisson ratio ⌧⌧0.33 and density ⌧⌧2800kg/m^3.

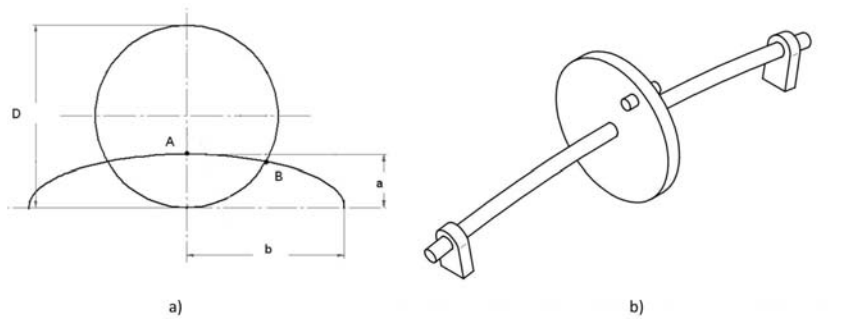


Figure 2: a) Geometry of the elliptical crack front; **b)** Jeffcott rotor model with an eccentric mass.

The aim of the present work is to evaluate the quasi-static behavior of the shaft (displacements and opening of the crack) at different angular positions of the rotation. Therefore, the analysis has been made considering a succession of static problems of the shaft with different angular positions of the crack with respect to the fixed reference axis. Even though the real problem is dynamic, here the static one is considered at each angular position in order to know the influence of both the eccentric mass and the position of the crack together. To develop the study eight different angular positions, one for every eighth of a rotation has been considered, called angle of rotation, ⊠⊠⊠⊠see Figure 3a. Then we analyze, at each angular position, the static behavior of the shaft considering the gravity effect.

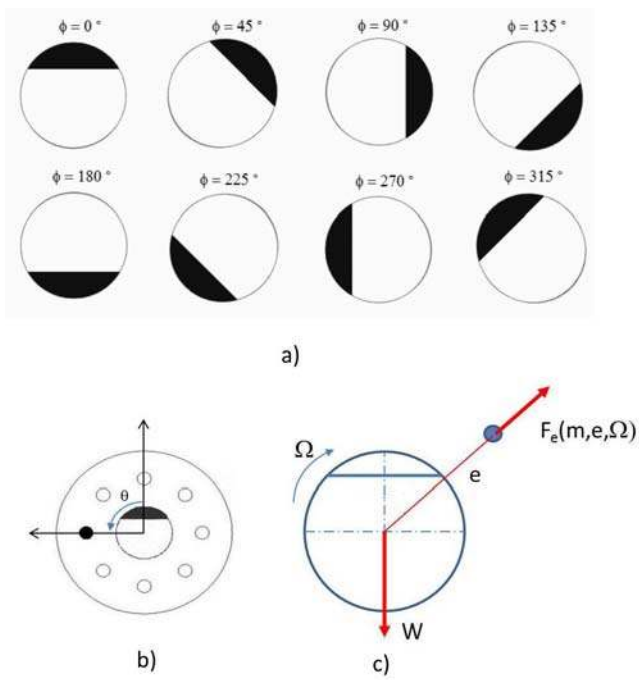


Figure 3: a) Angular positions, ⊠, of the crack during one rotation; **b)** Relative positions of the eccentricity with respect to the crack; **c)** Resume of the applied forces on the shaft.

As the intention of the paper is to study the effect of an unbalance on the opening of the crack, an eccentric mass has been placed on the disc of the Jeffcott rotor as an additional mass as shown in Figure 2b. The unbalance has been taken into account considering an eccentric mass m, located at a radial distance e from the center of the shaft, at the same longitudinal position of the crack, and with an angular position, ☒, with respect to the crack. This practice has been carried out by other authors (i. e. Bachschmid et al. 2008 or Kulesza et al. 2012) although in the first case the eccentric mass and crack are located in separate positions along the shaft. For that, the eccentric mass has been placed on the disc situated at different angles (angle of eccentricity ☒) measured from the position of the crack as shown in Figure 3b). The inertial force, F_e has been introduced in the quasi-static problem to simulate the effect of the eccentric mass, corresponding to the mass m located at a distance e from the center of disc rotating with the angular rotating velocity of the shaft ☒☒ (see Figure 3c). The values taken for the present analysis are m=0.2 kg, e=80mm and ☒☒= 1000 rpm. A gravitational force W, has also been included in the simulation.

3.1 Straight front crack model

Cracks of three nondimensional lengths, ☒=a/D, and straight fronts have been modeled to evaluate the influence of both the crack size and the position of the eccentricity in the behavior of the shaft. A total of 144 cases have been simulated and analyzed accordingly with the following:

- nondimensional crack length ☒ =0.1; 0.3; 0.5
- eccentricity angle ☒☒☒ 0^o; 45^o; 90^o; 135^o; 180^o
- rotation angle ☒☒☒ 0^o; 45^o; 90^o; 135^o; 180^o; 225^o; 270^o; 315^o

To simulate the balanced shaft, 24 cases corresponding to the same three crack lengths and eight rotation angles and no eccentricity, have also been modeled in order to compare with the corresponding unbalanced cases.

3.2 Elliptical front crack model

Cracks of the same lengths of previous section, and different elliptical shapes (shape ratio), ☒=*a*/*b* (being *a* and *b* the axis of the elliptical shape, Figure 1a), have been modeled to evaluate the influence of the same variables of the previous section together with the shape ratio.

A total of 544 cases have been simulated and analyzed accordingly with the following:

- nondimensional crack length ☒=0.1; 0.3; 0.5
- nondimensional crack shape (shape ratio) ☒=0; 0.25; 0.5; 0.75
- eccentricity angle ☒☒☒ 0^o; 45^o; 90^o; 135^o; 180^o
- rotation angle ☒= 0^o; 45^o; 90^o; 135^o; 180^o; 225^o; 270^o; 315^o

In order to simplify the results we have focused on the following 256 cases:

- for the smaller crack, ☒=0.1, the four shape ratios including the straight front have been considered as well as the eight angular positions and the five eccentricities. So, for the smaller crack, 160 cases have been simulated.
- for the medium and large cracks, ☒=0.3 and ☒=0.5, two shape ratios, eight angular positions and one eccentricity corresponding to 90^o, have been studied.

The reason for this selection is based on the fact that it is very interesting to know the behavior of the shaft with incipient or shallow cracks (☒=0.1). On the other hand, due to the results obtained for the straight crack, and that are explained in the next section, we have focused the study for elliptical cracks with eccentricity ☒☒90°. The intention is to evaluate if the same behavior as that for straight front takes place for shafts with cracks having elliptical fronts.

In order to compare the results with those corresponding to the unbalanced cases, 64 cases have also been modeled corresponding to the same three cases but with no eccentricity.

4 CRACK BREATHING

4.1 Breathing mechanism of a crack

The presence of the crack in a shaft modifies its mechanical behavior due to the changes introduced in the flexibility. So, it is very interesting to know the behavior of the crack when the shaft is rotating and so, it has been studied in different ways. The easiest one is to consider the crack open or closed (usually called the "switching model") that sometimes is good enough for the analysis. However, the real behavior of the crack must be represented by taking into account the gradual opening and closing of the crack as the shaft rotates (Jun et al. (1992), Darpe et al. (2004), Papadopoulos (2004), Patel and Darpe (2008), Bachschmid et al. (2008), Al- Shudeifat and Butcher (2011)). This gradual opening and closing of the crack (see Figure 4) depends on the stress condition of the shaft at the cracked section. Both the Stress Intensity Factor at the crack front at each instant, that depends on the crack opening, and the amount of crack opening can be used to determinate the change in the flexibility of the shaft for other applications.

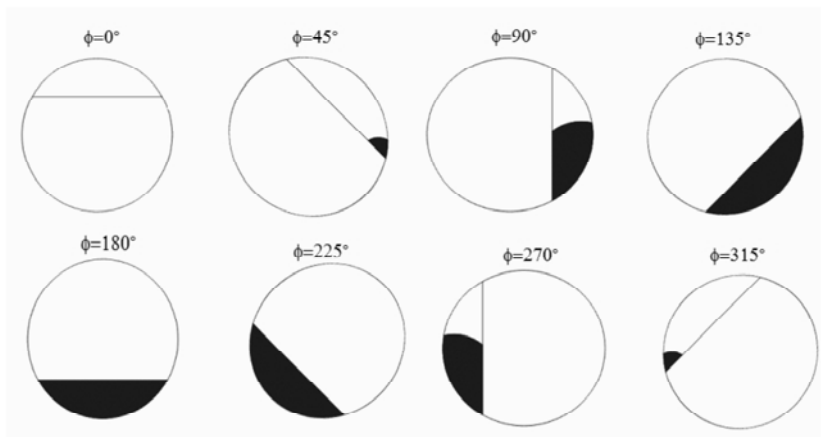


Figure 4: Crack breathing (open part in black) for a balanced shaft with ☒=0.3 in a full rotation.

4.2 Calculation of the crack opening

To analyze the breathing behavior of a crack during a rotation of the shaft, the aforementioned numerical simulations have been carried out. The study is focused on the opening of the cracked zone as the shaft rotates. In Figure 5 a detail of the cracked section, is shown. Here the opening of an elliptical crack with ☒=0.3 and ☒=0.5 can be observed. In this figure, the open part of the crack

is multi-colored while the close part is dark. The so obtained results are treated to be calculated using a software for the calculation of areas. From the multi-colored cracked surface, the border between the open part and the closed part can clearly be identified, and using a commercial code for solid modeling, the area of the open part can be given accurately. An example of the treatment of data is given in Figure 4. It shows the representation of the cracked section of a balanced shaft for a crack with ☒=0.3 and straight front, where the dark zone corresponds, in this case, to the open part of the crack during a rotation. Each image represents the situation for each of the rotation angles considered in the analysis.

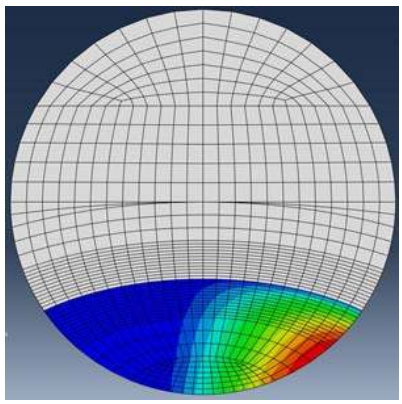


Figure 5: Detail of the cracked section with opening: closed part in dark, open part in multi-colors.

In order to analyze and to compare the results obtained for the different cases, the percentage of opening area has been derived as:

$$\Lambda = \frac{A_o}{A_c} \cdot 100 \tag{1}$$

where A_o is the calculated open cracked area for the current case, and A_c is the total cracked area independently of it is open or closed. The parameter ☒ that gives the percentage of open area will take values from 0 to 100, being 0 for the case of a completely closed crack and 100 for fully open cracks.

4.3 Crack opening of a straight crack

First of all, the results of the percentage of open area, ☒, for a balanced shaft are plotted in Figure 6. Here ☒ has been plotted versus rotation angle, ☒, for the cases ☒☒☒ 0.1; 0.3 and 0.5. Data of Figure 6 correspond to those of Figure 5. It should be pointed out that while no eccentricity is introduced in the problem, the crack opens and closes with symmetry as the shaft rotates. For example, when the shaft reaches the rotation angle ☒ $=90^0$ the amount of open part is exactly the same as that when the shaft is in ☒ $=270^0$. It is also shown that the opening of the crack lasts greater proportionally as the crack is longer, this means that the crack remains open more time during the rotation as the crack is longer. The shaft with a crack of ☒☒☒ 0.5 has an opening of ☒ =40% or more between ☒ $=50^0$ and ☒ $=310^0$ that is around 260^0 of the rotation. However, the shaft with the

crack of ⊠⊠⊠ 0.3 will be with the same opening between ⊠ =75^0 and ⊠ =285^0, that is around 210^0 of the rotation, smaller than the aforementioned case. The results obtained and the curves plotted for the balanced shaft will be taken as a reference to analyze the effect of the unbalance.

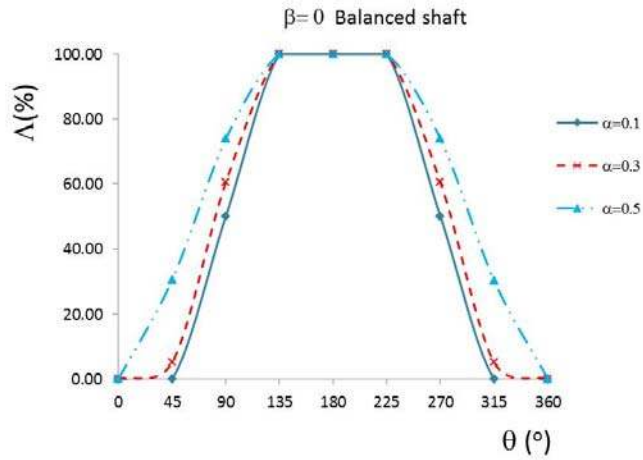


Figure 6: Percentage of opening of the crack in the balanced shaft in a rotation for different crack lengths. ⊠=0.

The effect of the eccentricity can be observed in Figure 7. Here the opening of the crack is shown for a selected rotation angle of ⊠ =270^0 for different eccentricity cases starting with the balanced (no eccentricity) shaft. There is a great difference of opening percentage depending on where the eccentric mass is located with respect to the crack. For the selected rotation angle and for the selected mass, m, distance to the center of the shaft, e, and rotation velocity, ⊠⊠ the shaft will remain closed (same as if the shaft was uncracked) if the mass is located just opposite to the crack (⊠=180^0), and will be fully open if the mass is in front of the crack (⊠=0^0), while if the eccentric mass is in between those angles, the crack will be partially open. A shaft with eccentricity, with an eccentricity angle of ⊠=90^0 , will present nearly the same open part as the balanced shaft.

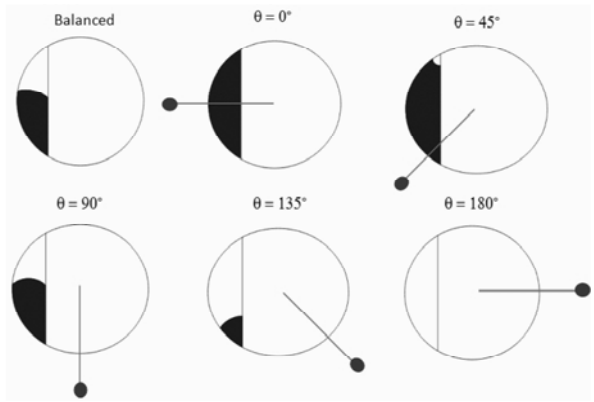


Figure 7: Crack breathing (open part in black) for different angles of eccentricity, ⊠. Case ⊠ =270^0 and ⊠⊠⊠ 0.3.

In Figure 8, the calculation of opening of the crack is shown for different values of the angle of eccentricity. The proportional open area is plotted against the rotation angle for different eccentricity angles for the cases ⊠⊠⊠ 0.1; 0.3 and 0.5, respectively.

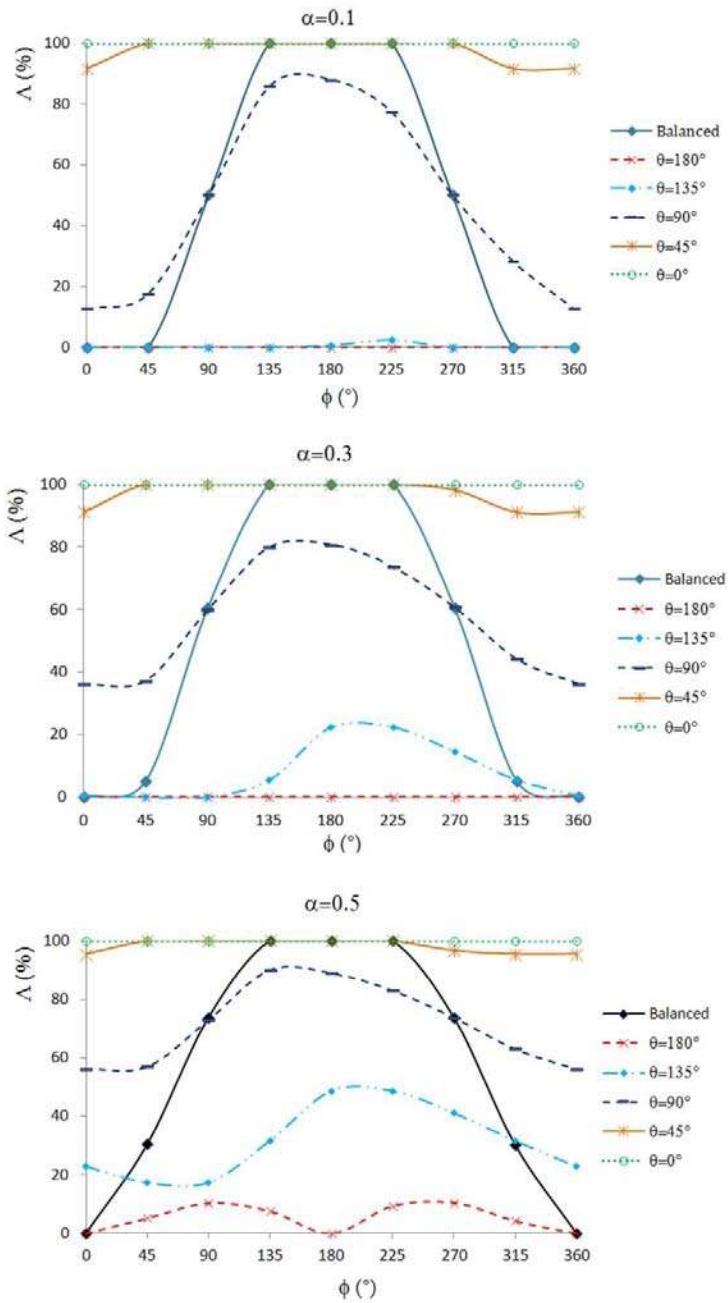


Figure 8: Percentage of opening of the crack in a rotation for different eccentricities. Case a) ⊠⊠⊠⊠0.1, Case b) ⊠⊠⊠⊠0.3, Case c) ⊠⊠⊠⊠0.5.

Looking to Figure 8 we can see that, for the selected m, e and ⊠, if the eccentricity is placed opposite to the crack (eccentricity angle ⊠=180^0, red line), the crack never opens while the crack is

small (□□□□0.1 and 0.3), which means that the cracked shaft behaves as it was an intact shaft. In this situation the crack will never propagate (the Stress Intensity Factor will be always null). The crack opens lightly if the crack is big (□□□□0.5). If the eccentric mass is at the same position as the crack (eccentricity angle □=0^0 , green dotted line) the crack will be always open independently of the length of the crack. In this situation the crack will be in a good position to propagate as the Stress Intensity Factor will take positive values. As the eccentric mass gets closer to the crack position (eccentricity angle between from 180^0 to 0^0), the shaft passes from having the crack always closed to having the crack always open. This trend is the same, independently, of the size of the crack. Nevertheless, the amount of opening and the time the crack remains open is greater as the crack is longer.

Another trend that can be observed through the figures is that as the eccentric mass gets closer to the crack position (eccentricity angle changing from 180^0 to 0^0), the maximum amount of opening (the peak of the curve) is reached for a smaller rotation angle. This happens with no dependency of the length of the crack.

There is an angle of eccentricity that needs a special attention because the crack is partially open for the whole rotation (never is fully open and never is fully closed) with no dependence of the crack length, and that is □=90^0.

As mentioned before, the percentage of opening increases with the length of the crack. In fact, for a deep crack □□□ 0.5 (Figure 8c)), the crack is partially open most of time of the rotation even for the maximum of the eccentricity angle.

4.4 Crack opening of an elliptical crack

Although the failures of rotating shafts sometimes are produced with more than one initiation front, it is very interesting to analyze the breathing mechanism of a single crack having an elliptical front shape, as they are the most feasible crack fronts in rotating shafts. In Figure 9, an example of the variation of the opening of the crack is shown for the case □□□ 0.5 and □□□ 0.5 in a full rotation.

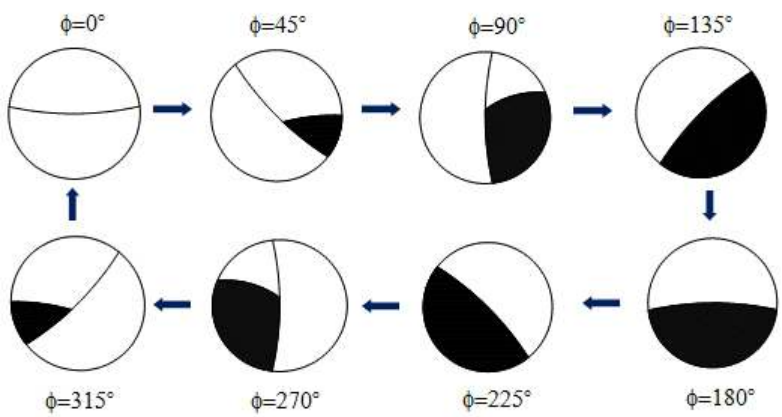


Figure 9: Crack breathing (open part in black) for a balanced shaft in a full rotation. Case □□□□0.5 and □□□□0.5.

Again, firstly the results for a balanced shaft are plotted in Figure 10. Here, the percentage of opening ☒ has been plotted versus angle of rotation ☒ for the three values of ☒☒and ☒=0.5. This figure shows the same trend of symmetry as that for the straight crack shown previously, while no eccentricity is introduced in the problem. In a whole rotation, the crack is sometimes fully closed and sometimes is fully open. So in approximately half the rotation, the crack is partially open. This breathing behavior pattern is the same for the different crack lengths but, it can be observed that for a selected angle of rotation, the opening of the crack is greater proportionally as the crack is longer. Another observation is that as the crack gets longer the part of the rotation in which the crack is open is greater, in fact a crack of ☒☒=0.5 never closes except for the angle ☒=0^0. The observed results, in the case of balanced shafts, are similar to those for straight cracks.

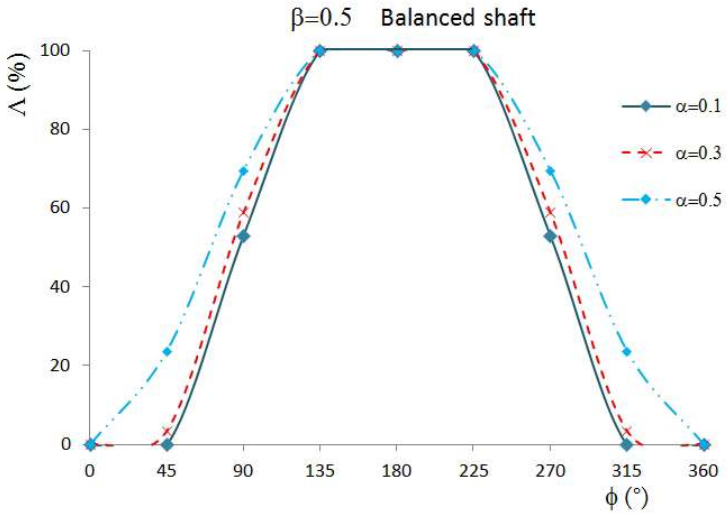


Figure 10: Percentage of opening of the crack in a balanced shaft in a rotation for different crack lengths for ☒☒☒0.5.

When the eccentric mass is introduced in the problem the same behavior is observed as for the straight cracks. In Figure 11, a comparison of the behavior for a balanced and an unbalanced (☒=90^0) shaft is shown. In this case, the properties of the crack are ☒=0.3 and ☒=0.5. The evolution of the breathing of the crack is compared in both situations. As can be seen, when an eccentric mass is considered in an angle of ☒=90^0 with respect to the crack position for a crack of medium length (☒=0.3), the crack is never fully closed neither fully opened. It is always partially open and the percentage of opening is around half of the crack all over the rotation. The balanced shaft is, in this case, more than one third of the rotation fully closed, one third of the rotation fully open and the other third partially open. A very important difference in the behavior has been detected between the balanced and the unbalanced cracked shaft, being the presence of an eccentric mass a source of changes in the breathing behavior of the shaft.

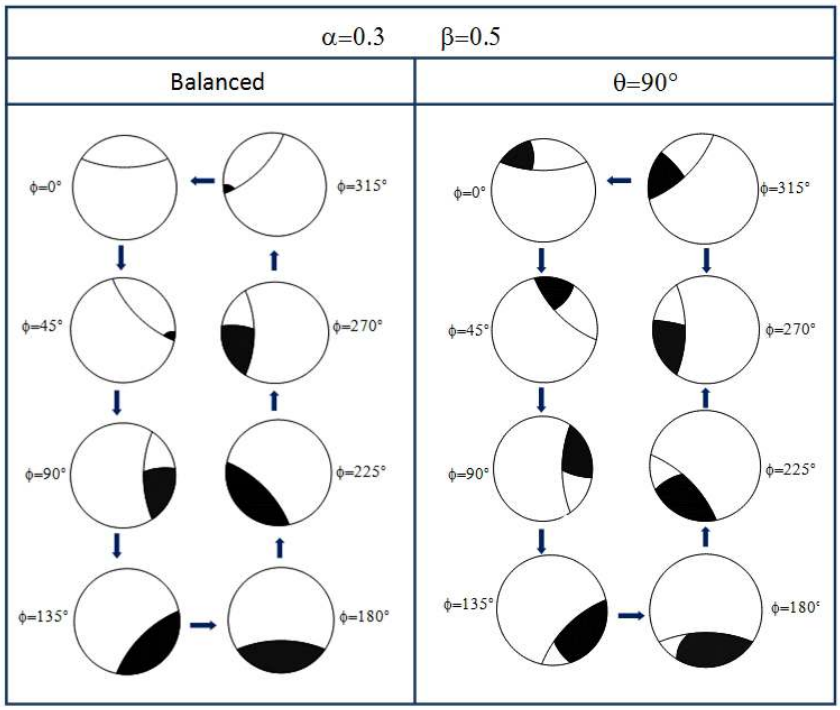


Figure 11: Comparison of the breathing mechanism in a rotation **a)** balanced shaft and **b)** unbalanced shaft. Case ⊠⊠⊠0.3 and ⊠⊠⊠⊠0.5.

As mentioned before, the study of shallow cracks is very interesting as they are the incipient cracks that will propagate to failure. The knowledge of the behavior of these cracks will allow us to detect them before they grow to a dangerous situation. Due to this, the analysis has been focused on cracks with ⊠⊠⊠0.1, widely considered small cracks in the scientific literature, in balanced and unbalanced (for different angles of eccentricity) shafts and for a complete rotation. In order to know the effect of the shape of the crack front, different shape ratios have also been considered. In Figure 12, the proportional open area is plotted against the rotation angle for different eccentricity angles and for the four shape ratios ⊠⊠⊠⊠0; 0.25; 0.5; 0.75.

It can be pointed out that for the selected eccentricity parameters m, e, rotation velocity ⊠⊠ and crack length ⊠, and for any of the values of shape ratio ⊠, if the eccentricity is placed opposite to the crack (eccentricity angle ⊠=180^0 , red line), the crack never opens, which means that the cracked shaft behaves as it was an intact shaft. In this situation the crack will never propagate (the Stress Intensity Factor will be null), the same as it happens to be for the straight crack. If the eccentric mass is at the same position as the crack (eccentricity angle ⊠=0^0, green dotted line) the crack will be always open and it will probably propagate as the Stress Intensity Factor would take positive values and could overcome the critical value called Fracture Toughness. If the eccentric mass is placed somewhere between the opposite side and the front side of the crack (eccentricity angle between 180^0 to 0^0), the shaft passes from having the crack always closed to always open. In the intermediate position of the eccentric mass, ⊠=90^0, the crack is partially open during the entire rotation for the shortest shape ratios ⊠=0 (in fact the straight front) and ⊠=0.25. As the shape

ratios are greater the percentage of opening gets similar to that of the balanced shaft during the rotation, being practically equal to that of the balanced shaft for⊠=0.75. All this can be observed n Figure 12.

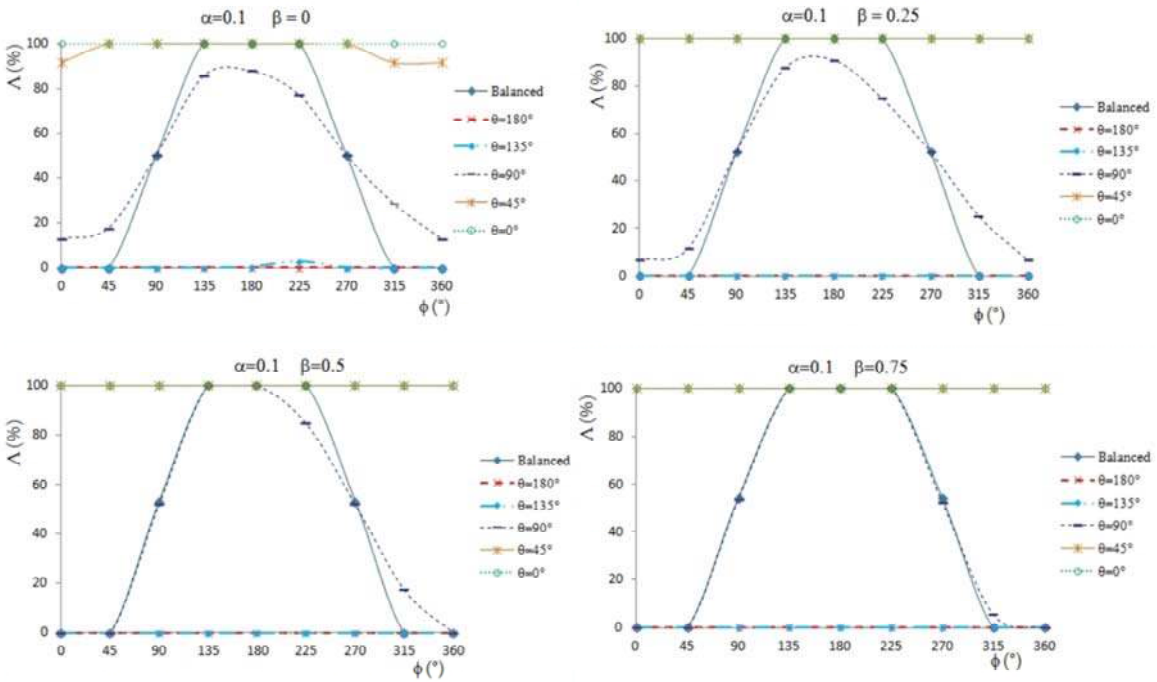


Figure 12: Percentage of opening of the crack in a rotation for different eccentricities for ⊠⊠⊠0.1.
a) Case ⊠⊠⊠⊠0; **b)** Case ⊠⊠⊠⊠0.25; **c)** Case ⊠⊠⊠⊠0.5; **d)** Case ⊠⊠⊠⊠0.75.

A comparison of the opening of the crack for the location ⊠=90^0 is shown in Figure 13. In this figure, the opening of the crack of ⊠=0.1 is plotted during a rotation for the different values of the shape ratio. Looking to the curves, a change in the pattern of the breathing can be observed with ⊠. While the angle of rotation is between ⊠=270^0 and ⊠=90^0 the less the shape factor, the more the opening of the crack. That means that as the crack is less elliptical, the percentage of opening is greater. Once the rotation passes through ⊠=90^0 the situation reverses and the less the shape factor (front more straight), the less the opening of the crack. This behavior is maintained up to ⊠=270^0. It is also observed that the maximum of the opening (the peak of the curve) is reached at lower angles of rotation as the shape factor takes greater values.

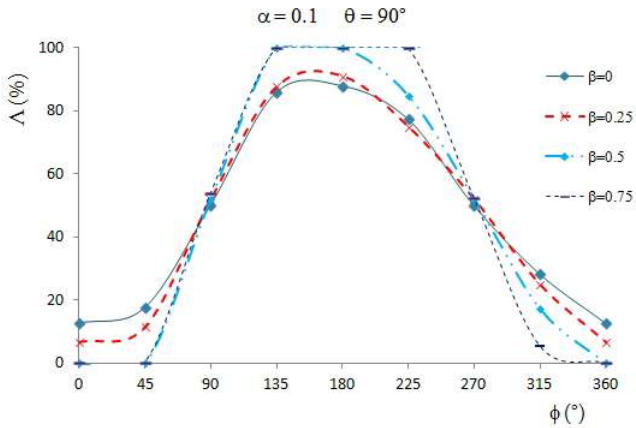


Figure 13: Percentage of opening of the crack in a rotation for ☒☒☒0.1 and ☒=90^0 for different shape ratios.

In Figure 14, a comparison of the opening of the cracks with ☒=0.5 for the analyzed eccentricity (☒=90^0) and for different crack lengths is shown. As can be seen, the medium and large cracks have a similar behavior (always partially open during the rotation) showing curves of the same shape, with percentages of opening that increase and decrease, relatively, at the same angle of rotation, being greater, proportionally, the opening of the large cracks. However, for the small cracks (☒=0.1) the trend is not similar, showing a different opening pattern. First of all the crack is closed in part of the rotation, and after that the relative opening is greater than for the deeper cracks reaching a complete opening in part of the rotation. This difference in the behavior of the small cracks can be explained taking into account that ☒ gives the relative open area (the area of the open crack with respect to the area of the crack). For the small cracks, it seems that it is not possible to find a situation in which the crack can be partially open or partially closed during the whole rotation. It seems that it is more difficult for a small crack to change its current opening or closing situation, but when the change from open to closed, or viceversa, is produced the opening or closing tends to be total.

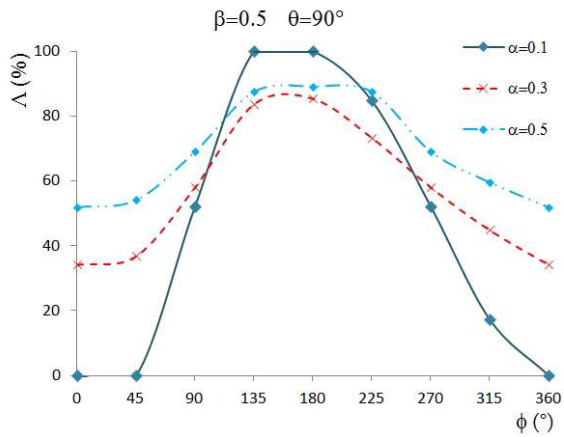


Figure 14: Percentage of opening of the crack in a rotation for ☒=90^0 for different crack lengths.

5 CONCLUDING REMARKS

It is very extended, for the case of rotating cracked shafts, the use of parameters obtained with their quasi-static behavior, such as the flexibility, the stress intensity factor or even the breathing mechanism of the crack, among others. In general, those parameters are considered for balanced shafts, although in many cases there are unbalances and misalignments. The results achieved in this work try to fill the gap of obtaining the same quasi-static parameters adding the problem of an unbalance. We incorporate the presence of an eccentric mass to analyze, as a previous step, the behavior of a quasi-static unbalanced rotating cracked shaft. It is clear that the results given here are not the dynamic results of rotating shafts, being only applicable for low rotating speeds, but as in the case of balanced cracked shafts they can give some information of the behavior of an unbalanced cracked rotating shaft to be used in preliminary studies on dynamics. As a result, a quasi-static numerical study of the effect that the presence of an eccentric mass and its orientation have on the breathing mechanism of a crack in a rotating shaft has been presented. Two different kinds of cracks have been considered: straight and elliptical cracks, through the shape ratio factor ☒=a/b taking values from 0 (straight crack) to 0.75 (nearly circular crack). Three crack lengths, eight rotation angles and five eccentricity positions have been analyzed. The very well-known Jeffcott rotor model has been used for the study. From the numerical results, obtained for given values of the eccentricity set (mass m, and distance e), and for a given speed velocity ☒☒ we can conclude that the percentage of opening increases with the length of the crack. Regarding the position of the eccentricity, if the eccentric mass is located opposite to the crack (☒=180^0) and if the crack is small (☒☒=0.1), the crack never opens and, consequently, the Stress Intensity Factor will be zero and the crack will not propagate. On the other hand, if the eccentric mass is situated in front of the crack (☒=0^0), the crack will be always open and very likely will propagate (only if the Stress Intensity Factor overcomes the critical value). For positions of the eccentricity between those mentioned, the opening and closing of the crack will depend on the angle of eccentricity, the crack length and the angle of rotation. There is a trend that appears independently of the crack length and the shape ratio: as the eccentric mass gets closer to the crack position the maximum amount of opening (the highest value of the curves) is reached with a smaller rotation angle.

A study for small cracks (☒☒=0.1) for an intermediate eccentricity (☒=90^0) and different shape ratios has been developed. The observed results shown that a change in the behavior is produced when the shaft passes through the angles of rotation ☒=90^0 and ☒=270^0. Between those angles, as the crack is more elliptical (increasing ☒☒ there is more percentage of crack open for the same angle of rotation. Out of these angles the situation is just the opposite. For these small cracks with little shape ratios the opening of the crack is determined by the angle of eccentricity more that by the angle of rotation. In fact, for the mentioned angle of eccentricity ☒=90^0, the straight (or nearly straight) small cracks are always partially open (they never open or close completely) but as they take the elliptical shape they open or close completely sometimes during the rotation.

Most of the crack or defect identification procedures are based on the dynamic behavior of the elements. The behavior or a cracked shaft is slightly different if the crack presents an elliptical shape (very frequent) that if the crack is straight (very less frequent). For maintenance purposes it is very interesting to know the behavior with the most feasible crack shape. The crack propagation,

and the crack propagation speed, depends on the stress intensity factor which depends itself very much on the variation of crack front shape.

The work allows us to know the influence of the unbalance of rotating shafts on the crack breathing mechanism and will help to predict the influence of this behavior on the values of the Stress Intensity Factor and, consequently, on the propagation of the cracks.

Acknowledgements

The authors gratefully acknowledge the financial support given by the Spanish Ministerio de Economía y Competitividad, through the Project DPI2009-13264, for the development of this work.

References

ABAQUS, (2007). Theory Manual (Version 6.7), Dassault Systemes Inc.

Al-Shudeifat, M.A., Butcher, E.A., (2011). New breathing functions for the transverse breathing crack of the cracked rotorsystem: approach for critical and subcritical harmonic analysis, Journal of Sound and Vibration 330: 526-544.

Bachschmid, N., Pennacchi, P., Tanzi, E., Smith, J., (2008). Some remarks on breathing mechanism, on non-linear effects an on slant and helicoidal cracks, Mechanical System and Signal Processing 22: 879-904.

Carpinteri, A., Brighenti, R., Spagnoli, A., (1998). Surface flaws in cylindrical shafts under rotary bending, Fatigue and Fracture of Engineering Materials and Structures 21: 1027-1035.

Cheng, L., Li, N., Chen, X.F., He, Z.J., (2011). The influence of crack breathing and imbalance orientation angle on the characteristics of the critical speed of a cracked rotor, Journal of Sound and Vibration 330: 2031-2048.

Couroneau, N., Royer, J., (1998). Simplified model for the fatigue growth analysis of surface cracks in round bars under mode I, International Journal of Fatigue 20: 711-718.

Darpe, A.K., Gupta, K., Chawla, A. (2004). Transient response and breathing behaviour of a cracked Jeffcott rotor. Journal of Sound and Vibration, 272: 207-243.

Darpe, A.K., Gupta, K., Chawla, A., (2006). Dynamics of a bowed rotor with a transverse surface crack, Journal of Sound and Vibration 296: 888-907.

Darpe, A.K., (2007). A novel way to detect transverse surface crack in a rotating shaft, Journal of Sound and Vibration 305: 151-171.

Dimarogonas, A.D., Papadopoulos, C.A., (1983). Vibration of cracked shafts in bending, Journal of Sound and Vibration 91: 583-593.

Gasch, R., (1976). Dynamic behaviour of a simple rotor with a cross sectional crack, Transactions of the IMechE. In: Proceedings of the International Conference on Vibration in Rotating Machinery Paper C178/76:123-128.

Gasch, R., (2008). Dynamic behaviour of the Laval rotor with a transverse crack, Mechanical System and Signal Processing 22: 790-804.

Gomez-Mancilla, J.C., Sinou, J.J., Nosov, V.R., Thouverez, F., Zambrano, A., (2004). The influence of crack-imbalance orientation and orbital evolution for an extended craked Jeffcott rotor, Comptes Rendus Mecanique 332: 955-962.

Gyekenyesi, A.L., Sawicki, J.T., Haase, W.C., (2010). Modeling disk cracks in rotors by utilizing speed dependent eccentricity, Journal of Materials Engineering and Performance 19: 207-212.

Ishida, Y., (2008). Cracked rotors: Industrial machine case histories and nonlinear effects shown by simple Jeffcott rotor, Mechanical System and Signal Processing 22: 805-817.

Jun, O.S., Eun, H.J., Earmme, Y.Y., Lee, C.W., (1992). Modelling and vibration analysis of a simple rotor with breathing crack, Journal of Sound and Vibration 155: 273-290.

Jun, O.S., Gadala, M.S., (2008). Dynamic behaviour analysis of a cracked rotor, Journal of Sound and Vibration 309: 210-245.

Kulesza, Z., Sawicki, J.T., (2012). Rigid finite element model of a cracked rotor, Journal of Sound and Vibration 331: 4145-4169.

Morais, T.S., Steffen, V., Mahfoud, J., (2012). Control of the breathing mechanism of a cracked rotor by using electro-magnetic actuator: numerical study, Latin American Journal of Solids and Structures 9: 581-596.

Muller, P.C., Bajowski, J., Soffker, D., (1994). Chaotic and fault-detection in a cracked rotor, Nonlinear Dynamics 5: 233-254.

Muñoz-Abella, B., Rubio, L., Rubio, P., Montero, L., (2012). Study of the breathing mechanism of an elliptical crack in a rotating shaft with an eccentric mass, in: Proceedings of the World Congress on Computational Mechanics, Sao Paulo, Brasil.

Papadopoulos, C.A., Dimarogonas, A.D., (1987). Coupled longitudinal and vertical vibrations of a rotating shaft with an open crack, Journal of Sound and Vibration 117: 81-93.

Papadopoulos, C.A., (2008). The strain energy release approach for modelling cracks in rotors: a state of the art review, Mechanical System and Signal Processing 22: 763-789.

Papadopoulos, C.A., (2004). Some comments on the calculation of the local flexibility of cracked shafts, Journal of Sound and Vibration 278: 1205-1211.

Patel, T.H., Darpe, A.K.,(2008). Influence of crack breathing model on nonlinear dynamics of a cracked rotor, Journal of Sound and Vibration 311: 1953-1972.

Patel, T.H., Zuo, M.J., Darpe, A.K., (2011). Vibration response of a coupled rotor systems with crack and misaligment, Proceedings of the IMechE Part C: Journal of Mechanical Engineering Science 225: 700-713.

Penny, J.E.T., Friswell, M.I., (2002). Simplified modelling of rotor cracks, in: Proceedings of ISMA, International Conference on Noise and Vibration Engineering 2: 607-615, Leuven, Belgium.

Pu, Y.P., Chen, J., Zou, J., Zhong, P. (2002). Quasi-periodic vibration of cracked rotor on flexible bearings, Journal of Sound and Vibration 251: 875-890.

Qin, W., Meng, G., Zhang, T., (2003). The swing vibration, transverse oscillation of cracked rotor and the intermittence chaos, Journal of Sound and Vibration 259: 571-583.

Qin, W., Cheng, G., Ren, X., (2004). Grazing bifurcation in the response of cracked Jeffcott rotor, Nonlinear Dynamics 35: 147-157.

Qingkai, H., Hongliang, Y., Bangchun, W., (2010): Parameter identifications for a rotor system based on its finite element model and with varying speeds, Acta Mechanica Sinica 26: 299-303.

Rubio, L., Muñoz-Abella, B., Loaiza, G. (2011). Static behaviour of a shaft with an elliptical crack, Mechanical System and Signal Processing 25: 1674-1686.

Rubio, L., Muñoz-Abella, B., Rubio, P., Montero, L. (2012). Influence of the eccentricity in the crack breathing in a rotating shaft, in: Proceedings of 8th International Conference on Engineering Computational Technology (ECT). Croatia.

Rubio, P. (2014). Factor de intensidad de tensiones en fisuras elípticas con mecanismo de apertura y cierre en ejes giratorios, Ph.D. Thesis (in Spanish). Univesity Carlos III of Madrid, Spain.

Sekhar, A.S., Prabhu, B.S., (1998). Condition monitoring of cracked rotors through transient response, Mechanism and Machine Theory 33: 1167-1175.

Shin, C.S., Cai, C.Q., (2004). Experimental and finite element analyses on stress intensity factors of an elliptical surface crack in a circular shaft under tension and bending, International Journal of Fracture 129: 239-264.

Zhou, T., Sun, Z., Xu, J., Han, W., (2005). Experimental analysis of a cracked rotor, Journal of Dynamic Systems Measurement and Control 127: 313-320.